J. Phys. Chem. A **2002,** *106,* 1374−1380

Atom Scrambling of Linear C_5 in the Gas Phase: a Joint Experimental and Theoretical Study

Suresh Dua and John H. Bowie*

Department of Chemistry, The University of Adelaide, South Australia, 5005

Received: August 7, 2001; In Final Form: November 5, 2001

The radical anion $[CC^{13}CCC]^{-\bullet}$, with known bond connectivity, has been synthesized in the ion source of a VG ZAB 2HF mass spectrometer by the reaction of $(CH_3)_3Si-C\equiv C^{13}C(=NNH\text{-tosyl})\text{-}C\equiv C-Si(CH_3)_3$ with HO^- followed by F^- (from SF_6). The collision-induced mass spectrum of $[CC^{13}CCC]^{-\bullet}$ shows only one fragmentation: exclusive loss of ^{12}C. Computational studies at the CCSD(T)/aug-cc-pVDZ//B3LYP/6-31G-(d) level of theory indicate that this experimental observation means that $[CC^{13}CCC]^{-\bullet}$ does not rearrange under the conditions of collisional activation. The charge reversal [$^-CR^+$, synchronous charge stripping of the radical anion (by a vertical Franck−Condon process) to the radical cation], and the neutralization/reionization [$^-NR^+$, stepwise vertical oxidation of the radical anion to the neutral, then of the neutral to the radical cation] spectra of $[CC^{13}CCC]^{-\bullet}$ show partial and complete atom scrambling, respectively. Under the experimental conditions used, the neutral has a lifetime of 10^{-6} s before being converted to the corresponding radical cation. Computational studies at the CCSD(T)/aug-cc-pVDZ//B3LYP/6-31G(d) level of theory suggest that the major atom-scrambling pathway of the neutral involves cyclization of singlet $CC^{13}CCC$ to equilibrating and degenerate carbon-substituted rhombic structures that fragment to yield linear singlet $^{13}C^{12}C_4$ structures. Overall, the label is randomized. A similar mechanism is proposed to account for the partial atom scrambling of the radical cations formed in the $^-CR^+$ experiment from $[CC^{13}CCC]^{-\bullet}$.

Introduction

Small carbon clusters are present in the stellar medium[1] and are considered[2,3] to be the precursors of large carbon molecules[4,5] including aromatic species and fullerenes.[6] To date, C_2, C_3, and C_5 are the only small carbon neutrals definitely identified in the stellar medium; e.g,. in the circumstellar envelope of the evolved carbon star IRC+10216.[7] In addition to their astrochemical significance, carbon clusters and their ions play important roles in combustion chemistry,[8] together with catalysis and material sciences.[9] A range of linear and cyclic carbon clusters have been made by several techniques, and have been characterized.[2,3,10−21]

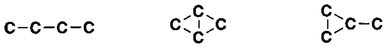
A ($D_{\infty h}$) **B** (D_{2h}) **C** (C_{2v})

We have synthesized some small carbon clusters by converting negative ions of known bond connectivity into neutrals in a mass spectrometer, and by using reionization of the neutrals as a probe to study the structures of those neutrals. This method is known as the neutralization/reionization technique (^-NR).[22] For example, we have shown experimentally that the energized and linear cumulene C_4 (**A**), after formation from linear $C_4^{-\bullet}$, equilibrates the four carbon atoms, and theory suggests that equilibration of the carbons is a consequence of rearrangement through the rhombus C_4 (**B**).[23] Rhombus C_4 has been a controversial species since 1977, when it was first proposed that neutral C_4 may have a planar cyclic ground state.[24] Recent theoretical studies have confirmed that linear C_4 (**A**) and rhombus C_4 (**B**) have similar energies, with the remaining 'low-energy' C_4 structure being the three-membered ring structure **C**, calculated to have a singlet ground-state structure some 27 kcal mol^{-1} above **B**.[23]

SCHEME 1

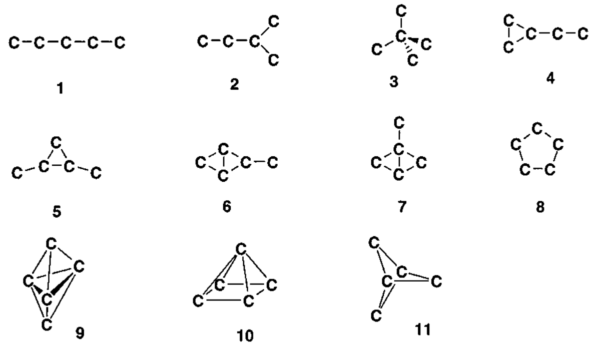

The C_5 molecule detected in star system IRC+10216 is reported to be the linear cumulene **1** (Scheme 1).[7] Linear C_5 has also been studied in a MINDO/2 study,[24] and by electronic spectroscopy.[25] Some possible C_5 isomers are shown in Scheme 1. (Scheme 1 shows only geometries and bond connectivities; bond orders are not indicated.) Some of these structures, viz **1**, **3**, **5**, **8**, **9,** and **10** have been studied by using theoretical calculations (e.g., refs 27−31). Of the structures studied, cumulene **1** is reported to be the most stable by some 60 kcal mol^{-1}; structures **5**, **8,** and **9** are of comparable energy (60, 67, and 66 kcal mol^{-1} with respect to **1** at the MP2/D95* level of theory), whereas structures **3** and **10** are not stable at this level of theory.[27] No experimental report of the formation of any other C_5 isomer exists apart from **1**. No calculations have been reported for the rhomboid structures **6** and **7**, even though rhombus C_4 (**B**) is a stable species.

This article addresses (*i*) the formation of linear C_5 from the radical anion analogue, and whether the neutral C_5 scrambles

---

*Corresponding author. E-mail: john.bowie@adelaide.edu.au.

10.1021/jp013060f CCC: $22.00

the C atoms (like the lower homologue linear C_4) when the system is energized, and (*ii*) if carbon equilibration does occur, what is the mechanism of that rearrangement?

Experimental Section

A. Mass Spectrometric Methods. For a detailed description of the experiment and the instrument used, see ref 31. In brief, the experiments were performed using a two-sector modified VG ZAB 2HF mass spectrometer with BE configuration, where B and E represent magnetic and electric sectors, respectively. The $C_5^{-\bullet}$ anion was generated by chemical ionization (CI) in the negative ion mode, with typical source conditions as follows: source temperature, 200 °C; repeller voltage, −0.5 V; ion extraction voltage, 7 kV; mass resolution, $m/\Delta m \geq 1500$. The precursor 1,5-bis(trimethylsilyl)-3-^{13}C-penta-1,4-yne-3-*p*-tosyl hydrazone was placed in a small glass capillary tube, which was then drawn out in a flame to create a very fine aperture, allowing for a slow steady release of sample vapor upon heating. The capillary was inserted into the CI source via the direct probe; the probe tip was heated to 60−80 °C to generate a background pressure of ca. 10^{-5} Torr inside the source housing. The $C_5^{-\bullet}$ anion was formed as shown in Scheme 3, using a 1:1 mixture of H_2O and SF_6 as CI reagent gases (to liberate the reagent ions HO^- and F^- respectively) at a pressure of ca. 10^{-4} Torr inside the source housing.

Collisional-induced dissociation (CID) of B mass selected ions was effected in the first of the two tandem collision cells positioned between B and E. Argon was used as a target gas. The pressure of the collision gas in the cell was maintained such that 80% of the parent ion beam was transmitted through the cell. This corresponds to an average of 1.1−1.2 collisions per ion.[32] Product ions resulting from CID were recorded by scanning E.

Neutralization-reionization[22] ($^-$NR$^+$) experiments were performed for B mass-selected $C_5^{-\bullet}$ by using the dual-collision cells located between sectors B and E. Neutralization of the anions was achieved by collisional electron detachment with O_2 at 80% transmittance as collision gas, whereas reionization to cations was achieved by collision of the neutrals with O_2, again at 80% transmittance. Any ions remaining after the first collision event were deflected from the primary neutral beam with an electrode maintained at a high voltage (1.5 kV) positioned before the second collision cell.

To detect a reionization signal due to the parent, the neutral species must be stable for approximately 1 μs. Charge reversal ($^-$CR$^+$) spectra[33,34] were recorded by using single collision conditions in collision cell 1 (O_2, 80% T).

B. Synthesis of the Labeled Precursor. Prepared by reported procedures.[35,36] $^{13}C = 99.5\%$.

C. Theoretical Methods. Geometry optimizations were performed with the Becke 3LYP method[37,38] using a modest 6-31G(d) basis within the GAUSSIAN 98 suite of programs.[39] Stationary points were characterized as either minima (no imaginary frequencies) or transition structures (one imaginary frequency) by calculation of the frequencies with use of analytical gradient procedures. The minima connected by a given transition structure were confirmed by intrinsic reaction coordinate (IRC) calculations. The calculated frequencies were also used to determine zero-point vibrational energies, which were then scaled[40] by 0.9804 and used as a zero-point correction for the electronic energies calculated at this and higher levels of theory. B3LYP/6-31G(d) has previously been used for geometry optimizations of anionic carbon clusters and has demonstrated good correlation with structures calculated with high-level, coupled-cluster approaches.[41,42] Some problems have been highlighted in the literature regarding the use of the B3LYP method for the accurate prediction of molecular energies for carbon clusters,[43] even though the method continues to be used with success.[29,30] Consequently, more accurate energies for the B3LYP geometries were determined with the CCSD(T) method[44−49] together with the Dunning aug-cc-pVDZ basis set.[50,51] The CCSD(T)/aug-cc-pVDZ//B3LYP/6-31G(d) approach predicts the adiabatic electron affinity of linear C_4 to be 3.65 eV, which is in reasonable agreement with the experimentally measured value of 3.88 eV.[52,53] A reviewer has questioned the accuracy of this method [see ref 54 and Table 8 (supplementary data)]. All calculations were performed on Power Challenge Supercomputers at either the South Australian Supercomputing Centre (Adelaide) or the Australian National University Supercomputing Facility (Canberra).

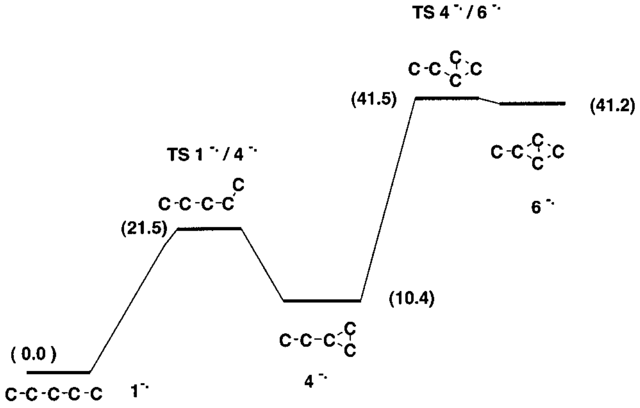

Figure 1. Calculated pathway for conversion of $1^{-\bullet}$ through $4^{-\bullet}$ to $6^{-\bullet}$ on the anion potential energy surface. The energies are given in kcal mol^{-1} with respect to $1^{-\bullet}$ (0 kcal mol^{-1}) and are calculated at the CCSD(T)/aug-cc-pVDZ//B3LYP/6-31G(d) level of theory. Full details of all structures shown in this figure are given in Table 1.

Results and Discussion

Isomeric C_5 Radical Anions: Theoretical Considerations. Before we embark upon a synthesis of the linear C_5 radical anion, we need to ascertain from a theoretical viewpoint whether this radical anion will be stable on formation in the ion source of the mass spectrometer. Theoretical calculations at the CCSD(T)/aug-cc-pVDZ//B3LYP/6-31G(d) level of theory of the radical anions of all the neutrals shown in Scheme 1 indicate that there are only three stable $C_5^{-\bullet}$ isomers of low energy: those corresponding to **1**, **4**, and **6** (see Scheme 2 and Table 1).

SCHEME 2

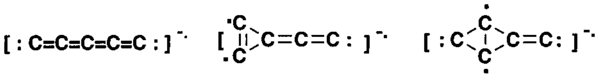

$1^{-\bullet}$ (0.0 kcal mol^{-1}) $4^{-\bullet}$ (+10.4) $6^{-\bullet}$ (+41.2)

Representations of the three radical anion isomers, $\mathbf{1}^{-\bullet}$, $\mathbf{4}^{-\bullet}$, and $\mathbf{6}^{-\bullet}$, are shown in Scheme 2, with full details of their energies and geometries listed in Table 1. The linear C_5 radical anion $\mathbf{1}^{-\bullet}$ is the global minimum on the anion potential surface, with $\mathbf{4}^{-\bullet}$ and the rhombic structure $\mathbf{6}^{-\bullet}$ being more positive in energy than $\mathbf{1}^{-\bullet}$ by 10.4 and 41.2 kcal mol^{-1}, respectively.

In Figure 1, we show the results of calculations [at the CCSD(T)/aug-cc-pVDZ//B3LYP/6-31G(d) level of theory] for the possible isomerization of the radical anion $\mathbf{1}^{-\bullet}$ through $\mathbf{4}^{-\bullet}$ to $\mathbf{6}^{-\bullet}$. Full details of the geometries and energies of $\mathbf{1}^{-\bullet}$, $\mathbf{4}^{-\bullet}$, and $\mathbf{6}^{-\bullet}$ and the two transition states are listed in Table 1. The barrier

TABLE 1: Minima and Transition States on the C5 Anion Surface[a]

	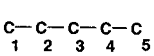	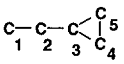	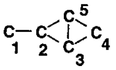	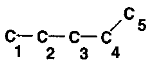	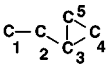
	$1^{-\bullet}$	**$4^{-\bullet}$**	**$6^{-\bullet}$**	**TS ($1^{-\bullet}$/$4^{-\bullet}$)**	TS (**$4^{-\bullet}$**/**$6^{-\bullet}$**)
state	$^{2}\Pi u$	$^{2}B_2$	$^{2}B_2$	–	$^{2}A'$
symmetry	$D_{\infty h}$	C_{2v}	C_{2v}	C_1	C_s
energy (hartree)	−189.774 89	−189.758 35	−189.709 28	−189.740 58	−189.708 77
rel energy (kcal mol^{-1})	0.0	10.4	41.2	21.5	41.5
bond lengths (Å)					
C_1C_2	1.290	1.270	1.416	1.305	1.317
C_1C_3			1.416		
C_2C_3	1.305	1.349	1.509	1.291	1.637
C_2C_4			1.490		
C_2C_5					1.410
C_3C_4		1.432	1.490	1.387	1.406
C_3C_5				2.065	1.523
C_4C_5		1.361	1.314	1.301	1.428
bond angles (°)					
$C_1C_2C_3$	180.0	180.0	120.1	180.0	144.2
$C_1C_2C_4$			117.4		
$C_2C_3C_4$		151.6	59.9		111.0
$C_2C_4C_5$			149.6		
$C_2C_5C_4$					124.5
$C_3C_4C_5$				140.3	
$C_1C_2C_3C_4$				197.8	
$C_2C_3C_4C_5$				−0.12	

[a] Geometries at the B3LYP/6-31G(d) level of theory, with single point energies (including zero point energy correction) at the CCSD(T)/aug-cc-pVDZ level. Anion radicals corresponding to **2**, **3**, **5**, **7**, **9,** and **10** (Scheme 1) are unstable at this level of theory. For details of **$8^{-\bullet}$** and **$11^{-\bullet}$** see supplementary data (Table 7).

for the conversion of **$1^{-\bullet}$** to **$4^{-\bullet}$** is 21.5 kcal mol^{-1}, whereas that for the formation of the rhombus isomer **$6^{-\bullet}$** is 41.5 kcal mol^{-1} at the level of calculation used. It is unlikely that either **$4^{-\bullet}$** or **$6^{-\bullet}$** could be formed from **$1^{-\bullet}$** in the ion-source under chemical ionization conditions.

Formation of Linear [CC^{13}CCC]$^{-\bullet}$ and the Collisional Activation Spectrum of This Species. The target species chosen for this study is [CC^{13}CCC]$^{-\bullet}$, and the key to the project is to find a method to prepare this anion radical. In principle, the synthesis looks straightforward, because we could use our SF_6 modification[23] of the Squires F^-/NF_3 S_N2 (Si) double-desilylation reaction[55] on the diazo compound **12** summarized in eq 1. Elimination of the two trimethylsilyl groups together with loss of dinitrogen should yield the required anion [CC^{13}CCC]$^{-\bullet}$.

$$(CH_3)_3Si{-}C{\equiv}C{-}^{13}C({=}N_2){-}C{\equiv}C{-}Si(CH_3)_3 + SF_6 \rightarrow \underset{(\mathbf{12})}{} \quad [CC^{13}CCC]^{-\bullet} + SF_4 + 2(CH_3)_3SiF + N_2 \quad (1)$$

The problem is that neutral precursor **12** is likely to detonate on heating in the direct inlet probe of the mass spectrometer. To avoid this possibility, we have used a process that has been used successfully in the condensed phase to liberate an $R_2C{=}N_2$ system in situ: namely, fragmentation of a deprotonated tosyl hydrazone.[36] The tosyl hydrazone **13** was synthesized from the ^{13}C-labeled ketone $(CH_3)_3Si{-}C{\equiv}C{-}^{13}C({=}O){-}C{\equiv}C{-}Si(CH_3)_3$.[36]

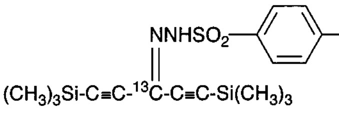

13

A plausible scenario to explain the formation of the required species [CC^{13}CCC]$^{-\bullet}$ from **13** is summarized in Scheme 3. Deprotonation of **13** with HO$^-$ in the ion source of the mass spectrometer yields the deprotonated sulfonyl hydrazone shown in Scheme 3. This species decomposes to yield the required neutral precursor **12** plus the sulfinyl anion *p*-$CH_3C_6H_4SO_2^-$ in the ion source of the mass spectrometer. Reaction of **12** with F^- (from SF_6) yields anion [CC^{13}CCC]$^{-\bullet}$. The order of the sequence of this process (summarized in Scheme 3) is not known, i.e., whether the S_N2(Si) processes follow or proceed or are accompanied by the loss of dinitrogen. Indeed, the intimate mechanism of the Squires double-desilylation process is not known with certainty.[55] Other major peaks co-occurring with that of [CC^{13}CCC]$^{-\bullet}$ are (**13**−H)$^-$, and *p*-$CH_3C_6H_4SO_2^-$, consistent with the overall process shown in Scheme 3.

SCHEME 3

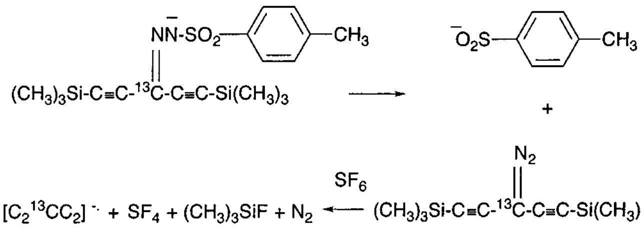

The collision-induced negative ion mass spectra of the ^{13}C-labeled C_5 radical anion with either Ar or O_2 as the collision gas are identical; the spectrum is shown in Figure 2. The sole fragment peak is produced by loss of ^{12}C from the molecular anion (cf., the exclusive loss of ^{13}C in the collisional activation spectrum of [$^{13}C{=}C{=}C{=}^{13}C$]$^{-\bullet}$ [23]), supporting the formulation of the ^{13}C-labeled C_5 radical anion as [CC^{13}CCC]$^{-\bullet}$.

Anion to Neutral Conversion. Although we have synthesized [CC^{13}CCC]$^{-\bullet}$ with known bond connectivity, the collision conditions used to effect Franck−Condon oxidative electron stripping of this anion to the corresponding neutral may, in principle, produce singlet or triplet neutral CC^{13}CCC. The geometries and energies of the C_5 neutrals have been calculated at the CCSD(T)/aug-cc-pVDZ//B3LYP/6-31G(d) level of theory; full results are summarized in Tables 2−4. The ground-state structure of CCCCC (**1**) is a singlet; the triplet is less stable by

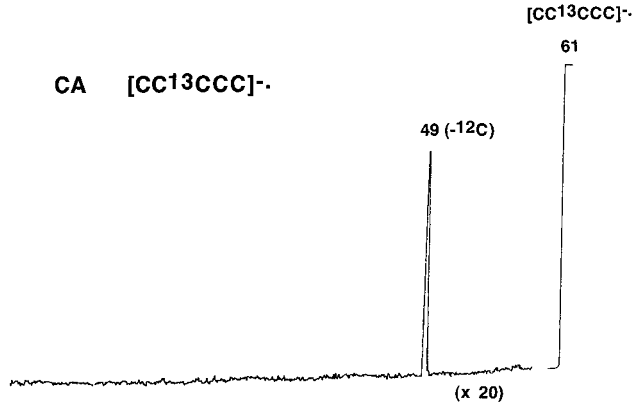

Figure 2. Collisional activation mass spectrum (MS/MS) of $[CC^{13}CCC]^{-\bullet}$. VG ZAB 2HF instrument. Collision gas, Ar. For experimental details, see Experimental Section.

TABLE 2: Energies of Anions, Neutrals and Cations of the C_5 Isomers 1−11 (Structures as in Scheme 1)[a]

structure	anion	singlet neutral	triplet neutral	cation
1	−189.774 89 (0)	−189.696 33 (0)	−189.591 509 5 (0)	−189.271 450 (0)
2	unstable (4)	unstable (**6**)	unstable (**4**)	unstable (**5**)
3	unstable (4)	unstable (**11**)	unstable (**4**)	unstable (**6**)
4	−189.758 35 (10.4)	unstable (**1**)	−189.585 174 (4.0)	-189.239 32 (20.2)
5	unstable (1)	−189.57960 (73.3)	−189.491250 (62.9)	−189.193410 (49.0)
6	−189.709 28 (41.2)	−189.608 92 (54.9)	unstable (**4**)	−189.230 38 (25.8)
7	unstable (6)	unstable (**6**)	unstable (**4**)	unstable (**6**)
8	−189.673 16 (63.8)	unstable (**5**)	−189.511 49 (50.2)	unstable (**12**)[b]
9	unstable (11)	unstable (**11**)	unstable (**10**)	unstable (**11**)
10	unstable (11)	unstable (**6**)	−189.472 89	unstable (**11**)
11	−189.648 35 (79.4)	−189.574 14 (76.7)	(74.4) unstable (**10**)	−189.156 55 (72.1)

[a] Energies (including zero-point correction) at the CCSD(T)/aug-cc-pVDZ//B3LYP/6-31G(d) level of theory. Relative energies with respect to that of the lowest energy isomer [$\mathbf{1}^{-\bullet}$, **1**, or $\mathbf{1}^{+\bullet}$ as appropriate (each 0.0 kcal mol^{-1})]. Unstable, in the context of this article, means that at the level of theory used, the proposed structure is not a stable minimum in its own right, but collapses to the isomeric structure that is indicated in parentheses. [b] See Figure 6, Table 5, and ref 58.

63.9 kcal mol^{-1}.[56] We are unable to control the energy of the collision-induced neutralization process, so the Franck−Condon vertical oxidation of linear $C_5^{-\bullet}$ may form both singlet and triplet CCCCC (**1**).

The charge reversal ($^{-}$CR^{+}) and neutralization-reionization ($^{-}$NR^{+}) mass spectra of $[CC^{13}CCC]^{-\bullet}$ are shown in Figures 3 and 4, respectively. Both spectra show scrambling of the carbon label, i.e., both species show losses of (*i*) ^{12}C and ^{13}C and (*ii*) $^{12}C_2$ and $^{12}C^{13}C$. The peak area ratios for ^{12}C and ^{13}C losses and $^{12}C_2$ to $^{12}C^{13}C$ losses in the $^{-}$CR^{+} experiment are 13.5:1 and 3.3:1, respectively, with maximum errors of ±5% in the area ratios. The corresponding peak area ratios in the $^{-}$NR^{+} spectrum are 3.9:1 and 1.45:1, with maximum errors of ±10% in the peak area measurements. The calculated values for total scrambling are 4:1 and 1.5:1; these calculations take no account of the mechanism(s) of scrambling. Scrambling is less in the $^{-}$CR^{+} spectrum. The CR process involves synchronous vertical Franck−Condon conversion of the anion to the cation, and fragmentation can immediately follow cation formation. In contrast, scrambling is complete under $^{-}$NR^{+} conditions. The NR method involves a two-step process in which the transient neutral has a microsecond lifetime before conversion to the 'decomposing' radical cation. Thus, the neutral products formed by charge-stripping of $\mathbf{1}^{-\bullet}$ undergo scrambling of the carbon atoms during the lifetime (10^{-6} s) of the neutral in the $^{-}$NR^{+} experiment.

TABLE 3: Minima and Transition Structures on the C_5 Neutral Singlet Surface[a]

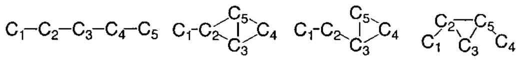

	^{1}**1**	^{1}**6**	TS ^{1}**1**/^{1}**6**	TS ^{1}**6**/^{1}**6**
state	$^1\Sigma g^+$	$^1A_1$	$^1A'$	$^1A_1$
symmetry	$D_{\infty h}$	C_{2v}	C_s	C_{2v}
energy (Hartrees)	−189.696 333 1	−189.608 92	−189.601 76	−189.596 31
rel. energy (kcal mol^{-1})	0.0	54.9	59.3	62.8
bond lengths (Å)				
C_1–C_2	1.292 (1.290)[b]	1.316	1.307	1.339
C_2–C_3	1.287 (1.282)[b]	1.439	1.351	1.466
C_3–C_4		1.439	1.353	1.657
C_4–C_5		1.427	1.460	1.339
C_2–C_5		1.427	1.742	1.408
C_3–C_5		1.482	1.523	1.466
bond angles (°)				
C_1–C_2–C_5		149.0	130.8	132.5
C_2–C_5–C_4		117.7	102.2	
C_1–C_2–C_3			171.8	72.2
C_2–C_3–C_4			135.0	

[a] Calculated at the B3LYP/6-31G(d) level of theory, with single-point energies (including zero-point energy correction) computed at CCSD(T)/aug-cc-pVDZ. The values given in parentheses represent the available literature data for comparison (see references for sources). [b] Calculated at CCSD(T)/cc-pVDZ level of theory.[28]

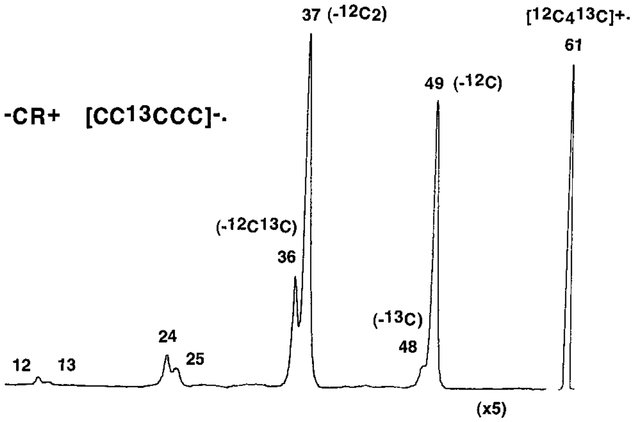

Figure 3. Charge reversal mass spectrum ($^{-}$CR^{+}) of $[CC^{13}CCC]^{-\bullet}$. VG ZAB 2HF instrument. Collision gas, Ar. For experimental details, see Experimental Section.

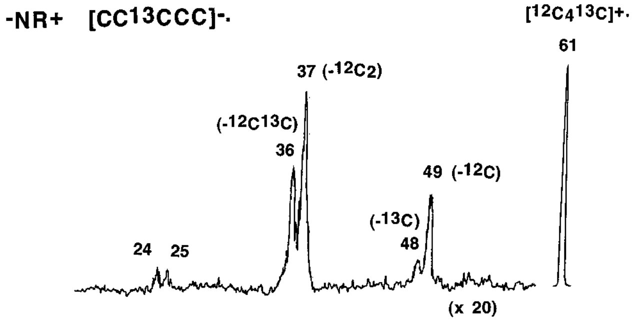

Figure 4. Neutralization/reionization mass spectrum ($^{-}$NR^{+}) of $[CC^{13}CCC]^{-\bullet}$. VG ZAB 2HF instrument. Collision gas in each cell, O_2. For experimental details, see Experimental Section.

TABLE 4: Minima and Transition Structures on the C_5 Neutral Triplet Surface[a]

	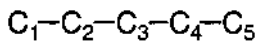	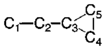	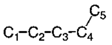	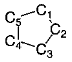	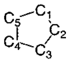
	^{3}**1**	^{3}**4**	TS ^{3}**1**/^{3}**4**	^{3}**8**	TS ^{3}**1**/^{3}**8**
state	$^3\Pi$g	$^3B_2$		^{3}A"	^{3}A"
symmetry	$D_{\infty h}$	C_{2v}	C_1	C_s	C_s
energy (Hartrees)	−189.591 51	−189.594 52	−189.562 21	−189.511 49	−189.457 78
rel. energy (kcal mol^{-1})	0.0	4.0	18.4	50.2	83.9
bond lengths (Å)					
C_1–C_2	1.268	1.284	1.311	1.309	1.290
C_2–C_3	1.299	1.319	1.306	1.391	1.411
C_3–C_4		1.449	1.360	1.392	1.387
C_4–C_5		1.364	1.324	1.311	1.343
				1.502	1.533
bond angles (°)					
C_2–C_3–C_4		151.9		112.0	103.7
C_3–C_4–C_5			96.01	105.1	107.8
C_1–C_2–C_3–C_4			178.4		
C_2–C_3–C_4–C_5			−1.6		

[a] Calculated at the B3LYP/6-31G(d) level of theory, with single-point energies (including zero-point energy correction) computed at CCSD(T)/aug-cc-pVDZ.

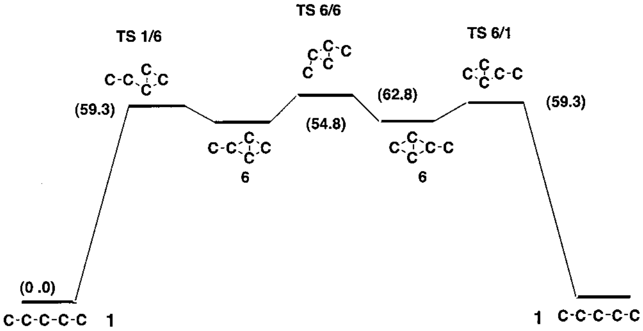

Figure 5. Calculated pathway for conversion of singlet CCCCC (**1**) through to equilibrating and degenerate forms of singlet rhombus C_5 (**6**). Energies are given in kcal mol^{-1} with respect to singlet CCCCC (0 kcal mol^{-1}) and are calculated at the CCSD(T)/aug-cc-pVDZ//B3LYP/6-31G(d) level of theory. Full details of structures are given in Tables 2−4.

Scrambling of the Carbons in Linear C_5. It is now necessary to return to Scheme 1 and consider which of the neutral C_5 structures could (*i*) be formed from **1** and (*ii*) account for the carbon scrambling observed experimentally. Because, in principle, singlet and triplet structures exist of the 11 isomers shown in Scheme 1, we have calculated, for comparison purposes, all 22 of these structures at the CCSD(T)/aug-cc-pVDZ//B3LYP/6-31G(d) level of theory. Energy data are summarized in Table 2. In principle, formation and subsequent fragmentation of any of **6** to **11** could account for the carbon scrambling. Some of these possibilities can be excluded after consideration of the data shown in Table 2; namely, (*i*) both the singlet and triplet forms of **7**, **9,** and **10** are unstable at the level of theory used, (*ii*) the triplet form of **11** is unstable at this level of theory, and (*iii*) the singlet form of **11** lies 105.5 kcal mol^{-1} above singlet **1** and is excluded on thermochemical grounds. We are now left with only two structures that might account for the atom scrambling, i.e., **6** and **8**, and of these, triplet **6** and singlet **8** are unstable at the level of theory used for the calculation. The following scenarios remain: (*i*) singlet CCCCC (**1**) scrambles the carbons by cyclization to the singlet rhombus **6**, and (*ii*) triplet CCCCC (**1**) scrambles the carbons by cyclization to triplet cyclo-C_5 (**8**).

The mechanisms for the scrambling of the carbon atoms of singlet and triplet C_5 have been investigated at the CCSD(T)/aug-cc-pVDZ//B3LYP/6-31G(d) level of theory. Summary data are shown in Figures 5 and 6, but full details of the structures shown in these figures are listed in Tables 2−4. The key feature of Figure 5 is that the scrambling of the carbons of singlet **1** proceeds by means of interconversion of the two degenerate rhombic C_5 structures **6**. The energy required to effect this overall sequence is 62.4 kcal mol^{-1}, which should be compared with the barrier of interconversion of linear C_4 through rhombus C_4 of 40 kcal mol^{-1}. The major difference between the two systems is the greater stability of rhombus C_4 than that of the carbon-substituted rhombus **6**. Even though the barrier required to effect formation of the rhombic C_5 structures is significant (+ 62.4 kcal mol^{-1}), this energy is much smaller than that required to cause decomposition of the linear C_5 system, namely, $C_5 \rightarrow C_4 + C$ (+230 kcal mol^{-1}), and $C_5 \rightarrow C_3 + C_2$ (+162 kcal mol^{-1}).[57]

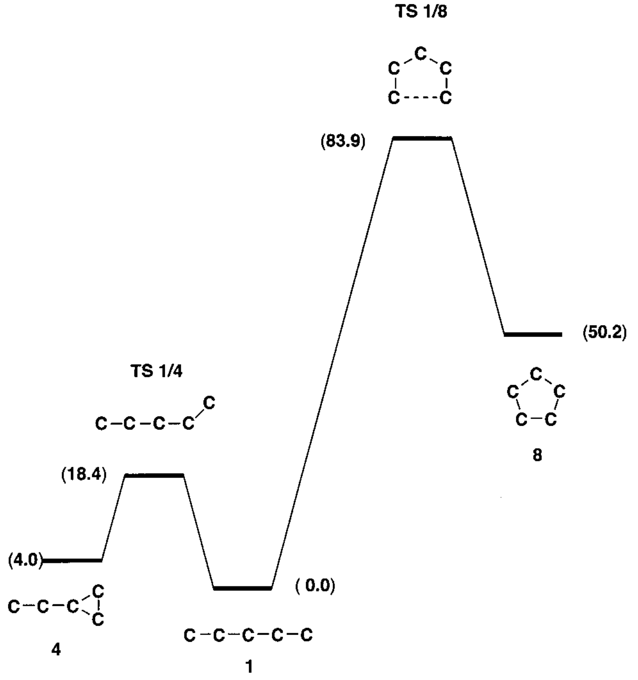

Figure 6. Calculated pathway for conversion of triplet CCCCC (1) and triplet CC-cyclo-C_3 (**4**) through triplet cyclic C_5 (**8**). Energies are given in kcal mol^{-1} with respect to triplet CCCCC (0 kcal mol^{-1}) and are calculated at the CCSD(T)/aug-cc-pVDZ//B3LYP/6-31G(d) level of theory. Full details of structures are given in Tables 2−4.

Charge stripping of $\mathbf{1}^{-\bullet}$ can also form the triplet neutrals **1** (see earlier). The interconversion of triplet **1** (and triplet **4**) to

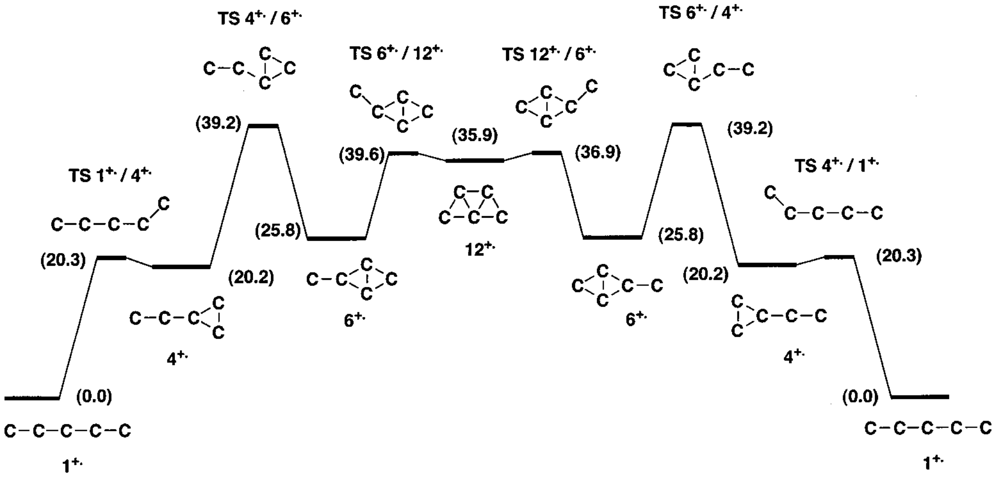

Figure 7. Calculated pathway for the conversion of $1^{+\bullet}$ through $4^{+\bullet}$ to equilibrating degenerate forms of $6^{+\bullet}$. Energies are given in kcal mol^{-1} with respect to $1^{+\bullet}$ (0 kcal mol^{-1}) and are calculated at the CCSD(T)/aug-cc-pVDZ//B3LYP/6-31G(d) level of theory. Full details of structures are given in Tables 2 and 5.

TABLE 5: Minima and Transition Structures on the C_5 Cation Surface[a]

	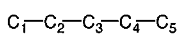	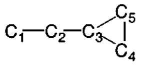	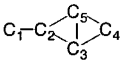	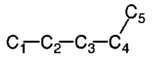	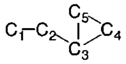	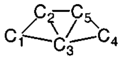	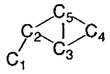
	$1^{+\bullet}$	$4^{+\bullet}$	$6^{+\bullet}$	TS $1^{+\bullet}/4^{+\bullet}$	TS $4^{+\bullet}/6^{+\bullet}$	$12^{+\bullet}$	TS $6^{+\bullet}/12^{+\bullet}$
state	$^2\Sigma$u	^{2}A″	^{2}A$_1$	^{2}A′	^{2}A′	^{2}A$_1$	
symmetry	$D_{\infty h}$	C$_s$	C_{2v}	C$_s$	C$_s$	C_{2v}	C_1
energy (Hartrees)	−189.271 45	−189.217 95	−189.230 38	−189.239 07	−189.209 03	−189.215 87	−189.214 24
rel. energy (kcal mol^{-1})	0.0	20.2	25.8	20.3	39.2	35.9	36.9
bond lengths (Å)							
C_1–C_2	1.271	1.317	1.344	1.324	1.324	1.321	1.324
C_2–C_3	1.290	1.298	1.443	1.276	1.336	1.487	1.479
C_3–C_4		1.470	1.348	1.415	1.316	1.490	1.400
C_4–C_5		1.317	1.348	1.306	1.361	1.321	1.333
C_2–C_5			1.443		1.949	1.446	1.431
C_3–C_5		1.477	1.531	1.653	1.668	1.487	1.512
bond angles (°)							
C_1–C_2–C_3		164.0	147.9	178.6	165.1	63.8	78.1
C_2–C_3–C_4		154.2	113.3	163.6	165.1	111.0	111.5
C_2–C_3–C_5		152.7			80.1	58.2	57.2
C_3–C_4–C_5				74.7	77.1		67.1

[a] Calculated at the B3LYP/6-31G(d) level of theory, with single-point energies (including zero-point energy correction) computed at CCSD(T)/aug-cc-pVDZ.

triplet cyclo C_5 (**8**) is shown in Figure 6. Interconversion of triplets **1** and **4** cannot effect carbon scrambling, but conversion of these through triplet **8** will. The barriers for these processes are shown in Figure 6. The barrier of 83.9 kcal mol^{-1} is significantly higher than the maximum barrier (62.4 kcal mol^{-1}) calculated for scrambling of singlet CCCCC. We could not find a lower-energy stepwise sequence for the interconversion of triplets **1** and **8**.

We conclude that the carbon scrambling of singlet CCCCC (**1**) occurs by cyclization to and equilibration of the singlet rhombic neutral **6**. In contrast, it is proposed that carbon scrambling of triplet CCCCC (**1**) is energetically unfavorable in comparison with carbon scrambling in singlet CCCCC; if the triplet neutral does undergo carbon scrambling, this may occur by cyclization of triplet CCCCC (**1**) to triplet cyclic C_5 (**8**) with subsequent fragmentation of the cyclic system.

Scrambling of the Linear C_5 Radical Cation. Partial carbon scrambling is a feature of the $^-$CR$^+$ mass spectrum of $[CC^{13}CCC]^{-\bullet}$. This may be due to a shorter lifetime of the decomposing cation than that of the corresponding neutral(s), and/or it may be due to a smaller propensity for scrambling of the radical cation. To investigate the latter scenario, we have studied the possible scrambling of this radical cation by computational studies. The data collected in Table 2 show that the only low-energy cations that could reasonably be involved in the scrambling processes of $1^{+\bullet}$ are $4^{+\bullet}$ and $6^{+\bullet}$. Calculations at the CCSD(T)/aug-cc-pVDZ//B3LYP/6-31G(d) level of theory (summarized in Figure 7; full details in Table 5) show that $1^{+\bullet}$ can convert through $4^{+\bullet}$ to the rhombus C_5 ($6^{+\bullet}$). If this process is reversible, it can account for only partial scrambling of the label in $[CC^{13}CCC]^{+\bullet}$. Complete carbon scrambling will occur after equilibration of two degenerate forms of rhombus $6^{+\bullet}$ through $12^{+\bullet}$ with subsequent ring opening to $1^{+\bullet}$ as shown in Figure 7.[57] The data shown in Figures 5 and 7 suggest that carbon scrambling is possible for both the singlet neutral $CC^{13}CCC$ and the radical cation $[CC^{13}CCC]^{+\bullet}$. Thus, the complete atom scrambling of the neutral (in comparison with partial atom scrambling of the radical cation) is likely to be a function of the longer lifetime (10^{-6} s) of the neutral.

Conclusions

The most likely rationale to explain the complete atom scrambling observed for energized neutral $CC^{13}CCC$ (**1**) in the $^-$NR$^+$ experiment is that it occurs principally for the singlet neutral and involves cyclization to, equilibration of, and decomposition of degenerate singlet rhomboid structures **6**. An analogous, but more complex process is proposed to rationalize the partial scrambling of $[CC^{13}CCC]^{+\bullet}$ noted in the $^{-}CR^{+}$ spectrum of $[CC^{13}CCC]^{-\bullet}$.

Acknowledgments. This project was funded by the Australian Research Council. One of us (S.D.) thanks ARC for a research associate stipend. We thank the Australian National University (Canberra) for a generous allocation of time on the Australian National University Supercomputing Facility.

Supporting Information Available: Tables 6 and 7 list geometry and energy data of all stable anions, neutrals, and cations of the C_5 isomers **1**−**11** not included in Tables 2−5. Table 6, ^{1}**4**, ^{3}**4**, $\mathbf{4}^{+\bullet}$, and $\mathbf{8}^{-\bullet}$, Table 7, ^{3}**10**, $^{2}\mathbf{11}^{-\bullet}$, ^{1}**11**, and $^{2}\mathbf{11}^{+\bullet}$. Table 8 contains data from calculations at two levels (see ref 54). This material is available free of charge via the Internet at http://pubs.acs.org.

References and Notes

(1) Ehrenfreund, P.; Foing, B. H. *Astron. Astrophys*. **1996,** *307*, L25.
(2) Helden, G. von; Kemper, P. R.; Gotts, N. G.; Bowers, M. T. *Science* **1993,** *259*, 1300.
(3) Helden, G. von; Gotts, N. G.; Bowers, M. T. *Nature* **1993,** *363*, 60.
(4) *The Application of Plasmas to Chemical Processing*; Baddour, R. F., Timmins, R. S., Eds.; MIT Press: Cambridge, MA, 1967.
(5) Jones, J. M.; Malcolm, R. P.; Thomas, K. M.; Botrell, S. H. *Carbon* **1996,** *34*, 231.
(6) Kroto, H. W.; Heath, J. R.; O'Brien, S. C.; Curl, R. F.; Smalley, R. E. *Nature (London)* **1985,** *318*, 162.
(7) Bernath, P. F.; Hinkle, K. H.; Keady, J. J. *Science* **1989,** *244*, 562.
(8) Kroto, H. W.; McKay, K. *Nature (London)* **1988,** *331*, 328.
(9) Levi Guyer, R.; Koshland, D. E. *Science* **1990,** *250*, 1640.
(10) Weltner, W.; Van Zee, R. J. *Chem. Rev.* **1989,** *89*, 1713.
(11) Raghavachari, A. N. *J. Chem. Phys.* **1990,** *93*, 2099.
(12) Adamowicz, L. *Chem. Phys. Lett*. **1991,** *182*, 45.
(13) Watts, J. D.; Bartlett, R. J. *J. Chem. Phys.* **1992,** *97*, 3445.
(14) Kranz, R. H.; Graham, W. R. M. *J. Chem. Phys.* **1992,** *97*, 2517; **1993,** *98*, 71; Kranz, R. H.; Rittby, C. M. L.; Graham, W. R. M. *J. Chem. Phys*. **1995,** *103*, 6841; **1996,** *105*, 5313.
(15) Heath, J. R.; Saykally, R. J. *On Clusters and Clustering*; Reynolds, P. J., Ed.; Elsevier: Amsterdam, 1993; p 7; Orden, A. V.; Saykally, R. J. *Chem. Rev.* **1998,** *98*, 2313.
(16) Schmatz, S.; Botschwina, P. *Chem. Phys. Lett.* **1995,** *235*, 8; **1995,** *245*, 136.
(17) Weltner, W.; Van Zee, R. J.; Li, S. *J. Phys. Chem.* **1995,** *99*, 6277.
(18) Schmatz, S.; Botschwina, P. *Int. J. Mass Spectrom. Ion Processes* **1995,** *149*/*150*, 621.
(19) Zhao, Y.; deBeer, E.; Xu, C.; Taylor, T.; Neumark, D. M. *J. Chem. Phys*. **1996,** *105*, 4905. Zhao, Y.; deBeer, E.; Neumark, D. M. *J. Chem. Phys*. **1996,** *105*, 2575.
(20) Maier, J. P. *Chem. Soc. Rev.* **1997,** *1*, 21.
(21) Blanksby, S. J.; Bowie, J. H. *Mass Spectrom. Rev.* **1999,** *18*, 131.
(22) Wesdemiotis, C. *Chem. Rev.* **1987,** *87*, 485. Zagorevskii, D. V.; Holmes, J. H. *Mass Spectrom. Rev*. **1994,** *13*, 133. Goldberg, N.; Schwarz, H. *Acc. Chem. Res*. **1994,** *27*, 347. For more recent reviews, including NR nomenclature, see Shalley, C. A.; Hornung, G.; Schröder, D.; Schwarz, H. *Int. J. Mass Spectrom. Ion Processes* **1998,** *172*, 181. Zagorevskii, D. V.; Holmes, J. L. *Mass Spectrom. Rev*. **1999,** *18*, 87.
(23) Blanksby, S. J.; Schröder, D.; Dua, S.; Bowie, J. H.; Schwarz, H. *J. Am. Chem. Soc*. **2000,** *122*, 7105; see also references therein.
(24) Slanina, Z.; Zahradnik, R. *J. Phys. Chem*. **1977,** *81*, 2252.
(25) Motylewski, T.; Vaizert, O.; Geisen, T. F.; Linnartz, H.; Maier, J. P. *J. Chem. Phys*. **1999,** *111*, 6161; see also references therein.
(26) Kohno, M.; Suzuki, S.; Shiromaru, H.; Achiba, Y. *J. Chem. Phys.* **1999,** *110*, 3781; see also references therein.
(27) Ewing, D. W.; Pfeiffer, G. V. *Chem. Phys. Lett*. **1987,** *134*, 413.
(28) Botschwina, P. *J. Chem. Phys.* **1994,** *101*, 853.
(29) Martin, J. M. L.; El-Yazal, J.; François, J.-P. *Chem. Phys. Lett.* **1995,** *242*, 570. Martin, J. M. L.; El-Yazal, J.; François, J.-P. *Chem. Phys. Lett*. **1996,** *252*, 9. Martin, J. L. M.; Taylor, P. R. *J. Phys. Chem.* **1996,** *100*, 6047.
(30) Pasqualini, E. E.; López, M. *Chem. Phys. Lett*. **2000,** *320*, 415.
(31) Peppe, S.; Blanksby, S. J.; Dua, S.; Bowie, J. H. *J. Phys. Chem. A* **2000,** *104*, 5817.
(32) Holmes, J. L. *Org. Mass Spectrom.* **1985,** *20*, 169.
(33) Bowie, J. H.; Blumenthal, T. *J. Am. Chem. Soc.* **1975,** *97*, 2959. Szulejko, J. E.; Bowie, J. H.; Howe, I.; Beynon, J. H. *Int J. Mass Spectrom. Ion Phys.* **1980,** *13*, 76.
(34) Bursey, M. M. *Mass Spectrom. Rev.* **1990,** *9*, 555.
(35) Albuts, A. H.; Wyberg, H. *J. Chem. Soc. Chem. Commun.* **1988,** 748.
(36) An, Y. Z.; Rubin, Y.; Schaller, C.; McElvany, S. W. *J. Org. Chem.* **1994,** *59*, 2927.
(37) Becke, A. D. *J. Phys. Chem.* **1993,** *98*, 5648.
(38) Stevens, P. J.; Devlin, F. J.; Chablowski, C. F.; Frisch, M. J. *J. Phys. Chem.* **1994,** *98*, 11623.
(39) Frisch, M. J.; Trucks, G. W.; Schlegel, H. B.; Gill, P. M. W.; Johnson, B. G.; Robb, M. A.; Cheeseman, J. R.; Keith, T.; Peterson, G. A.; Montgomery, J. A.; Raghavachari, K.; Al-Laham, M. A.; Zakrzewski, V. G.; Ortiz, J. V.; Foresman, J. B.; Peng, C. Y.; Ayala, P. Y.; Chen, W.; Wong, M. W.; Andres, J. L.; Replogle, E. S.; Gomperts, R.; Martin, R. L.; Fox, D. J.; Binkley, J. S.; Defrees, D. J.; Baker, J.; Stewart, J. P.; Head-Gordon, M.; Gonzales, C.; Pople, J. A. *Gaussian 94*, revision B3; Gaussian Inc.: Pittsburgh, PA, 1995.
(40) Wong, M. W. *Chem. Phys. Lett.* **1996,** *256*, 391.
(41) Blanksby, S. J.; Dua, S.; Bowie, J. H. *J. Phys Chem. A* **1999,** *103*, 5161.
(42) Crawford, T. D.; Stanton, J. F.; Saeh, J. C.; Schaefer, H. F., III. *J. Am. Chem. Soc.* **1999,** *121*, 1902.
(43) Plattner, D. A.; Houk, K. N. *J. Am. Chem. Soc*. **1995,** *117*, 4405.
(44) Cizek, J. *Adv. Chem. Phys.* **1969,** *14*, 35.
(45) Raghavachari, K.; Trucks, G. W.; Pople, J. A.; Head-Gordon, M. *Chem. Phys. Lett.* **1989,** *157*, 479.
(46) Hampel, C.; Peterson, K.; Werner, H.-J. *Chem. Phys. Lett*. **1992,** *190*, 1.
(47) Watts, J. D.; Gauss, J.; Bartlett, R. J. J. *J. Chem. Phys*. **1993,** *98*, 8718.
(48) Knowles, P. J.; Hampel, C.; Werner, H.-J. *J. Chem. Phys.* **1993,** *99*, 5219.
(49) Deegan, M. J. O.; Knowles, P. J. *Chem. Phys. Lett.* **1994,** *227*, 321.
(50) Dunning, T. H. *J. Chem. Phys.* **1989,** *90*, 1007.
(51) Woon, D. E.; Dunning, T. H. *J. Chem. Phys.* **1993,** *98*, 1358.
(52) Arnold, D. W.; Bradforth, S. E.; Kitsopoulos, T. N.; Neumark, D. M. *J. Chem. Phys*. **1991,** *95*, 8753.
(53) Xu, C.; Burton, G. R.; Taylor, T. R.; Neumark, D. M. *J. Chem. Phys*. **1997,** *107*, 3428.
(54) A reviewer has asked why we used the RCCSD(T)/aug-cc-pVDZ//B3LYP/aug-cc-pVDZ level of theory in a previous paper in this series,[41] whereas in this and other recent articles we use the CCSD(T)/aug-cc-pVDZ//B3LYP/6-31G(d) level of theory; the reviewer has indicated the former to be the more accurate (cf. also ref 29). The answer is that calculations at the B3LYP/6-31G(d) level are some 20% more economical of computer time, and, in our hands, give results not significantly different from those calculated at the 'higher' level. We have calculated structures and energies of selected anions, neutrals, and transition states (reported in this article) at the two levels of theory to allow direct comparison. These data are collected in Table 8 (Supporting Information), and clearly illustrate results that are not significantly different.
(55) Wenthold, P. G.; Hu, J.; Squires, R. R. *J. Am. Chem. Soc.* **1994,** *116*, 6961.
(56) This is in accord with theoretical data, which indicate that neutral linear cumulenes with an odd number of carbons have singlet ground states, whereas cumulenes with an even number of carbons have triplet ground states.[15,23]
(57) Individual values from http://webbook.nist.gov.
(58) The structural relationship between $\mathbf{12}^{+\bullet}$ and $\mathbf{8}^{+\bullet}$ is of interest. The cation radical of **8** (cyclo C_5) is unstable at the level of theory indicated in Table 2. Attempted computation of $\mathbf{8}^{+\bullet}$ results in reorganization of this structure to give stable $\mathbf{12}^{+\bullet}$, the reactive intermediate between the two degenerate forms of $\mathbf{6}^{+\bullet}$ shown in Figure 7. No stable neutral or radical anion forms of **12** exist.